Available online at www.sciencedirect.com
ScienceDirect
Journal of Hazardous Materials 153 (2008) 557–565
Journal of Hazardous Materials
www.elsevier.com/locate/jhazmat

Modeling and simulation of ammonia removal from purge gases of ammonia plants using a catalytic Pd–Ag membrane reactor

M.R. Rahimpour*, A. Asgari

Department of Chemical and Petroleum Engineering, College of Engineering, Shiraz University, Shiraz 71345, Iran

Received 4 January 2007; received in revised form 29 August 2007; accepted 30 August 2007
Available online 4 September 2007

Abstract

In this work, the removal of ammonia from synthesis purge gas of an ammonia plant has been investigated. Since the ammonia decomposition is thermodynamically limited, a membrane reactor is used for complete decomposition. A double pipe catalytic membrane reactor is used to remove ammonia from purge gas. The purge gas is flowing in the reaction side and is converted to hydrogen and nitrogen over nickel-alumina catalyst. The hydrogen is transferred through the Pd–Ag membrane of tube side to the shell side. A mathematical model including conservation of mass in the tube and shell side of reactor is proposed. The proposed model was solved numerically and the effects of different parameters on the rector performance were investigated. The effects of pressure, temperature, flow rate (sweep ratio), membrane thickness and reactor diameter have been investigated in the present study. Increasing ammonia conversion was observed by raising the temperature, sweep ratio and reducing membrane thickness. When the pressure increases, the decomposition is gone toward completion but, at low pressure the ammonia conversion in the outset of reactor is higher than other pressures, but complete destruction of the ammonia cannot be achieved. The proposed model can be used for design of an industrial catalytic membrane reactor for removal of ammonia from ammonia plant and reducing NO_x emissions.

Keywords: NO_x emissions; Purge gas; Ammonia plant; Catalytic reactor; Pd–Ag membrane

1. Introduction

Ammonia is used for production of urea, nitric acid and ammonium nitrate. It is produced from synthesis gas in a large scale. Ammonia is produced in three steps: desulphurization of natural gas, synthesis gas production from natural gas and ammonia synthesis. The purge gas from ammonia synthesis plant contains some ammonia. Owing to the eutrophication problem caused by ammonia, the environmental regulations in every country are becoming steadily more stringent [1]. According to the worldwide emphasis on eutrophication problem and the toxic property of ammonia on the living, the discharge of ammonia to aquifers is intensely focused. At high levels of ammonia, toxic effects can be observed. These may include the death of animals, birds, fish and death or low growth rate in plant. Long term effects may include shortened lifespan, reproductive problems, lowered fertility, and changes in appearance or behavior. Exposure to high levels of ammonia can cause irritation and serious burn on the skin and in the mouth, throat, lungs and eyes [2].

In some ammonia plants the synthesis purge gas is burned in primary reformer as fuel and NO_x is generated according to the following reactions:

$$NH_3 + O_2 \leftrightarrow NO_2 + \tfrac{3}{2}H_2 \quad (1)$$

$$NH_3 + \tfrac{1}{2}O_2 \leftrightarrow NO + \tfrac{3}{2}H_2 \quad (2)$$

In order to utilize this purge gas for burning in the primary reformer, NH_3 must be removed to prevent NO_x formation. The concentration of NH_3 in the purge gas may be as high as 2.27 mol%. Therefore in an ammonia plant, 1600 t of ammonia is burned per year and NO_x is formed. Table 1 summarizes purge gas compositions in an ammonia plant [3]. The chemical process industry has task of reducing greenhouse effect by devising new processes and finding solutions which should not produce pollutant. Absorption of ammonia by water cannot remove NH_3 perfectly and 400 ppm of ammonia remains in purge gas [4]. The purge gas in Shiraz petrochemical complex is used for recovery of argon. Therefore ammonia is removed from

* Corresponding author. Tel.: +98 711 2303071; fax: +98 711 6287294.
E-mail address: rahimpor@shirazu.ac.ir (M.R. Rahimpour).

0304-3894/$ – see front matter © 2007 Elsevier B.V. All rights reserved.
doi:10.1016/j.jhazmat.2007.08.095

Nomenclature

A	membrane area (cm^2)
d	tube diameter (cm)
E	activation energy
F_i^s	molar flow rate of component i in shell side (mol/s)
F_i^t	molar flow rate of component i in tube side (mol/s)
F_{in}^s	molar flow rate of sweep gas (mol/s)
F_{in}^t	molar flow rate of purge gas (mol/s)
k	reaction rate constant (mol/(m^3 s))
k_0	pre-exponential factor (mol/(m^3 s $Pa^{-0.674}$))
K_{eq}	equilibrium constant (Pa)
l	axial position in reactor (cm)
L	tube length (cm)
P_i	partial pressure of component i in reaction side (atm)
P_1	hydrogen partial pressure in reaction side (atm)
P_2	hydrogen partial pressure in shell side (atm)
Q_H	Permeation rate of hydrogen through the Pd–Ag membrane (mol/s)
Q_i	permeation rate of component i (mol/s)
Q_0	permeation rate constant (mol cm/(cm^2 s $atm^{1/2}$))
r_{NH_3}	ammonia decomposition rate (mol/(m^3 s))
R	universal gas constant (kJ/(mol K))
T	reaction temperature (K)
y_{if}	mole fraction of component i in feed

Greek symbols

β	exponential constant in rate equation
δ	membrane thickness (cm)
ν_i	reaction stoichiometry of component i
π	3.1416

purge gas feed by water in scrubbing tower at pressure about 74 kg/cm^2. At these conditions, scrubbed purge gas, containing around 100 ppm ammonia leaves the scrubber [5]. Another method is ammonia destruction in a conventional packed bed catalytic reactor according to the following reaction:

$$NH_3 \leftrightarrow \tfrac{1}{2}N_2 + \tfrac{3}{2}H_2 \quad (3)$$

Table 1
Specifications of ammonia plant purge gases in Razi petrochemical complex [3]

Plant specifications	Value
Number of ammonia units	2
Capacity per unit (t/day)	1000
Purge gas flow rate per unit (kg mol/h)	285
Total ammonia in purge gases (t/year)	1600
Purge gas streams pressure (bar)	108.9
Gas composition (mol%)	
N_2	19.36
H_2	58.15
NH_3	2.27
Ar	6.02
CH_4	14.2

Ammonia decomposition reaction is limited due to the high concentrations of H_2 and N_2 in purge gas at these conditions. Therefore a catalytic membrane reactor should be used. Membrane reactor can be used to increase conversion when the reaction is thermodynamically limited as well as to increase selectivity when multiple reactions are occurring.

Thermodynamically limited reactions are reactions where the equilibrium lies far to the left and there is little conversion. The membrane reactor is another technique for driving reversible reactions to the right toward completion in order to achieve very high conversions. These high conversions can be achieved by having one of the reaction products diffuse out of a permeable membrane. For reactions, which are thermodynamically limited, selective product removal or reactant addition may be used to increase conversion. One of the most important advantages of membrane reactors is the possibility of overcoming the limitation imposed by thermodynamic equilibrium. The presence of a perm-selective membrane in a reacting system modified, via the Lechatelier–Brown principle, the conversion that can be achieved by the system, to higher than the equilibrium value. As a result, the reverse reaction will not be able to take place, and the reaction will continue to proceed to the right toward completion.

The hydrogen molecule is small enough to diffuse through the small pores of the Pd–Ag membrane while N_2 and NH_3 cannot (pore size of membrane is 4 nm [4]). Gobina et al. [4] performed an experimental and theoretical study on removal of ammonia from gasification of coal in a Pd–Ag membrane catalytic bed reactor. They used the feed containing hydrogen, ammonia, water, H_2S, N_2, $CO + CO_2$, CH_4 and implemented the membrane possesses 100% permeability to hydrogen alone. Recently, Rahimpour and Lotfinejad presented dynamic model for a Pd–Ag membrane dual-type methanol synthesis reactor [6]. Alloying the palladium, especially with silver, leads to an increase of the hydrogen permeability. A maximum value of the hydrogen flow is reached for an alloy with approximately 23 wt% silver. Similar to Pd/Ag, other alloys, e.g. Pd/Y or Pd/Ce show high hydrogen permeability and good mechanical stability [7]. Palladium-based membranes have been used for decades in hydrogen extraction because of their high permeability and good surface properties and because palladium, like all metals, is 100% selective for hydrogen transport [8].

Consequently, the reaction continues to proceed to the right even for a small value of the equilibrium constant. Other potential use for this method is hydrogen recovery from ammonia plant purge gas. Catalytic membrane reactor have been the subject of numerous recent investigations such as steam reforming of methane [7,9–11], dehydrogenation reactions [12–15], partial oxidation of methanol synthesis [16,17].

The main object of this work is enhancement of ammonia decomposition in membrane reactor. In this system, the wall of reactor is coated with a hydrogen perm-selective membrane. The hydrogen partial pressure gradient is the driving force for hydrogen permeation from reacting gas to sweeping gas. The advantages of the concept will be discussed based on ammonia conversion profile along the reactor. The

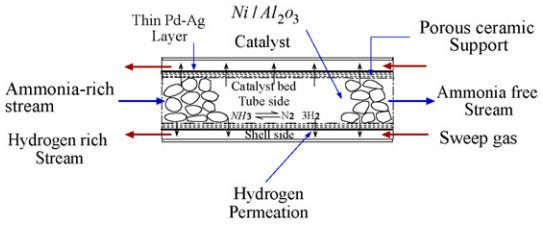

Fig. 1. Cross-section of a countercurrent flow catalyst bed membrane reactor.

results are compared with the performance of conventional-type reactor.

2. Reactor configuration

A schematic of catalytic membrane reactor for ammonia decomposition is shown in Fig. 1. NH_3 over Ni/Al_2O_3 catalyst converts to N_2 and H_2. This reactor is considered two concentric pipes. The inner pipe is catalytic reaction side and other pipe is shell side. The inner tube supports a dense film of Pd–Ag and the outer one is the non-permeable shell. The materials are flowing through the reaction and shell sides in co-current and counter-current flow modes. Hydrogen permeates along the reactor in order to control amount of hydrogen for better operability and efficiency.

3. Theory

3.1. Permeability of Pd–Ag membrane

The composite membrane used in this study is made of very thin layer of palladium–silver alloy. The membrane is deposited as a continuous layer on the outer surface of thermo stable support. The permeation rate of hydrogen through the Pd–Ag membrane [Q_H (mol/s)] is assumed to obey the half-power pressure law [18,19], then:

$$Q_H = Q_0(P_1^{1/2} - P_2^{1/2})\left(\frac{A}{\delta}\right) \quad (4)$$

where Q_0 is the permeability constant of hydrogen gas through the membrane (mol cm/(cm^2 s atm$^{1/2}$)); A is the membrane area available for flow (cm^2); and δ is the film thickness of the membrane (cm). The permeation rate of hydrogen is directly proportional to the difference in square roots of the upstream and downstream hydrogen partial pressures. The permeability constant of hydrogen gas (Q_0) through Pd–Ag film obey the Arrhenius law and can be expressed as follows [20,21]:

$$Q_0 = 3.2027 \times 10^{-9} \exp\left(\frac{-6.38}{RT}\right) \quad (5)$$

where R is universal gas constant (kJ/(mol K)) and T is absolute temperature (K).

3.2. Reaction kinetics

Ammonia decomposition/synthesis rate equation on a solid catalyst is assumed to obey Temkin–Phyzev mechanism [22]. Corresponding rate equation was generally accepted by many authors [23,24]. This reaction rate equation is:

$$r_{NH_3} = k\left[\left(\frac{P_{NH_3}^2}{P_{H_2}^3}\right)^{\beta} - \frac{P_{N_2}}{K_{eq}^2}\left(\frac{P_{H_2}^3}{P_{NH_3}^2}\right)^{1-\beta}\right] \quad (6)$$

where:

$$k = k_0 \exp\left(\frac{-E}{RT}\right) \quad (7)$$

The first term within the brackets of the rate equation is ammonia decomposition while the second term is the rate of ammonia synthesis. There are three kinetic parameters in the rate equation, the pre-exponential factor k_0 (mol/(m^3 s Pa$^{-0.674}$)), the activation energy E (J/mol) and β. These parameters were measured experimentally for NH_3 decomposition over Ni/Al_2O_3 catalyst on the pressure range 929–3549 kPa for a wide range of NH_3 and H_2 ratios [25]. A value of 0.674 was obtained for β. The resulting Arrhenius-type relationship for the rate constant is:

$$k = 5.744 \times 10^{19} \exp\left(\frac{-2.304 \times 10^5}{RT}\right) \quad (8)$$

The thermodynamic equilibrium constant K_{eq} defined by Harrison and Kobe according to the following equation [26]:

$$\log\left(\frac{1}{K_{eq}}\right) = \frac{2250.322}{T} - 0.8534 - 1.51049l \times \log T - 25.8987\times10^{-5}T + 14.8961 \times 10^{-8}T^2 \quad (9)$$

3.3. Model development

In order to represent membrane system, differential conservation of components equation was derived for co-current and countercurrent configurations. The equations were derived subject to the following assumptions:

1. Isothermal operation (due to low ammonia concentration).
2. Plug flow is considered in tube and shell side.
3. Pressure drop is negligible. The length of reactor is relatively small and the operating pressure is relatively high (36 atm).
4. Reaction occurs only inside catalyst bed (tube side).
5. Steady state operation.
6. One-dimensional flow is considered.

Although Gobina et al. [27,28] presented a rigorous model contains the concentrations as function of reactor length and radius, we considered one-dimensional model, because of the ratio of reactor length over reactor diameter is high (100/1 = 100) such as it is observed in Gobina et al. paper [4].

The mass balance equations in term of component molar flow are given in the following sections.

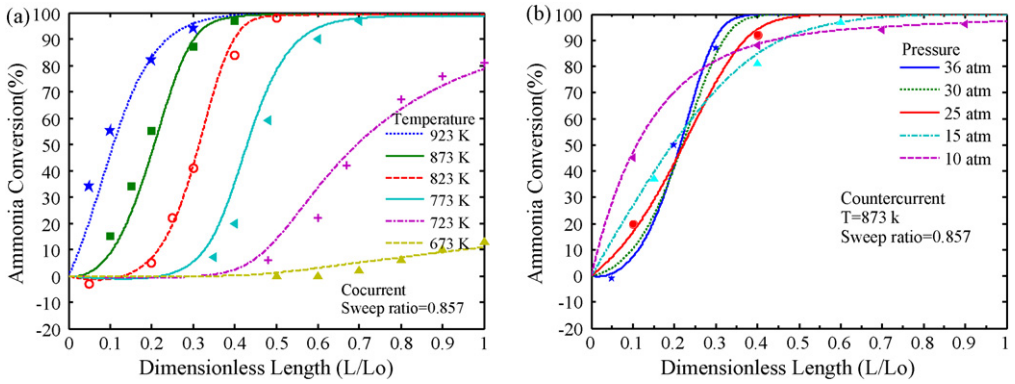

Fig. 2. Comparison of ammonia decomposition between model and Gobina data at different temperature and pressure: (a) co-current; (b) countercurrent.

3.4. Material balance

The model determines the molar flow rates of all components as a function of axial position in both the tube side and sweep side of the membrane reactor.

3.4.1. Tube side material balance

The differential material balance equations on species i for the tube side of both co-current and countercurrent flow catalytic membrane reactor are given below.

$$\frac{\mathrm{d}F_i^{\mathrm{t}}}{\mathrm{d}l} = \nu_i r_{\mathrm{NH_3}} \frac{\pi d^2}{4} - \frac{\mathrm{d}Q_i}{\mathrm{d}l} \tag{10}$$

The first term is the reaction term and the second term is the permeation term of species of i. ν_i is the reaction stoichiometry of each component (positive for product and negative for reactant). F_i^{t} is the component molar flow rate, l is axial position in reactor and d is the tube diameter.

3.4.2. Shell side material balance

A similar differential material balance equation is obtained for sweep side of the membrane reactor.

$$\frac{\mathrm{d}F_i^{\mathrm{s}}}{\mathrm{d}l} = \pm\frac{\mathrm{d}Q_i}{\mathrm{d}l} \tag{11}$$

The sign is positive for co-current and is negative for countercurrent flow. Four components are present in tube side, namely, ammonia, nitrogen, hydrogen and inert that consists of argon and methane.

4. Numerical solution

The model consists of six ordinary differential equations. The most widely used method of integration for ordinary differential equations are the series of methods called Runge–Kutta second, third and fourth order. We used the fourth order method for solving the system of equations. For co-current flow an initial value problem is solved since all boundary conditions are at the same point. The boundary conditions for co-current case for species i are:

$$F_i^{\mathrm{t}} = y_{i\mathrm{f}} F_{\mathrm{in}}^{\mathrm{t}} \qquad \text{at } l = 0 \tag{12}$$

$$F_i^{\mathrm{s}} = F_{\mathrm{in}}^{\mathrm{s}} \qquad \text{at } l = 0 \tag{13}$$

A boundary value problem is solved for the countercurrent flow since the tube and shell side boundary conditions are at opposite ends of the tube. The Shooting method converts the boundary value problem to an initial value one. In this method, the unspecified initial conditions of the differential equation system are guessed and the equations are integrated forward as a set of simultaneous initial value differential equations. At the end, the calculated final values are compared with the boundary conditions and the guessed initial conditions are corrected if necessary [29]. This procedure is repeated until the specified terminal values are achieved within small convergence criterion. Boundary conditions for countercurrent case for species i are:

$$F_i^{\mathrm{t}} = y_{i\mathrm{f}} F_{\mathrm{in}}^{\mathrm{t}} \qquad \text{at } l = 0 \tag{14}$$

$$F_i^{\mathrm{s}} = F_{\mathrm{in}}^{\mathrm{s}} \qquad \text{at } l = L \tag{15}$$

5. Model validation

The model was verified against results that were presented by Gobina et al. [4]. Fig. 2(a and b) and Table 2 show that there is insignificant error for co-current and countercurrent flow over the pressure range 10–36 atm and temperature range 673–923 K. Ammonia conversion along the reactor tube length is depicted in these figures. The base data for simulation in order to comparison are presented in Table 3. L/L_0 is the dimensionless reactor length and the specified points are experimental data.

Table 2
Comparison of ammonia decomposition between model and Gobina data at $T = 873$ K, $P = 36$ atm for countercurrent mode

Dimensionless length (L/L_0)	Ammonia conversion (%)		Error (%)
	Gobina data	Simulation results	
0.0625	3	3.07	2.3
0.125	18.4	18.57	1
0.35	93	92	1
0.625	100	99.6	0.6
1.0	100	100	0

Table 3
Input data for comparison between model and Gobina data [4]

Volume of the catalyst bed (cm^3)	6.689
Palladium–silver film thickness (cm)	6×10^{-4}
Diameter of catalyst pellets (cm)	0.15–0.2
Catalyst density (kg/m^3)	510
Surface area of catalyst (m^2/kg)	190,000
Void fraction	0.4
Pressure of synthesis gas (atm)	36.0
Pressure of sweep gas stream (atm)	1.0
Flow rate of synthesis gas (cm^3/min)	350.0
Flow rate of sweep gas (cm^3/min)	300.0
Tube length (cm)	14
Feed composition (mol%)	
H_2	20
NH_3	0.3
N_2	48
$CO + CO_2$	26
H_2O	1.5
CH_4	4.2

Table 4
Summary of input parameters used for catalytic membrane reactor simulation

Palladium–silver film thickness (cm)	6×10^{-4}
Diameter of catalyst pellets (cm)	0.15–0.2
Catalyst density (kg/m^3)	510
Surface area of catalyst (m^2/kg)	190,000
Void fraction	0.4
Pressure of sweep gas stream (atm)	1.0
Flow rate of synthesis gas (mol/min)	0.180
Flow rate of sweep gas stream (mol/min)	0.150
Tube diameter (cm)	1
Reactor and membrane length (cm)	100
Pressure of feed gas (atm)	36
Membrane surface area (cm^2)	314

6. Results and discussion

The effect of various parameters on NH_3 decomposition in a catalytic membrane reactor was investigated. Temperature, tube side pressure, sweep gas flow ratio, configuration of membrane, membrane thickness and membrane diameter are several options that was considered in reactor performance. The parameters used in the membrane reactor simulation are listed in Table 4. The composition of the inlet tube stream is based on the purge gas of Razi petrochemical complex in the ammonia plant (Table 1).

6.1. Comparison between equilibrium reactor and membrane reactor

Fig. 3 shows that the ammonia conversion in catalytic membrane reactor will be higher than equilibrium one if we choose the proper conditions. Ammonia conversion is defined as:

$$\text{Ammonia conversion} = \frac{F^{t}_{NH_3,in} - F^{t}_{NH_3,out}}{F^{t}_{NH_3,in}} \times 100 \qquad (16)$$

In lower temperatures the rate of ammonia decomposition is small and decreasing pressure of tube side decreases the

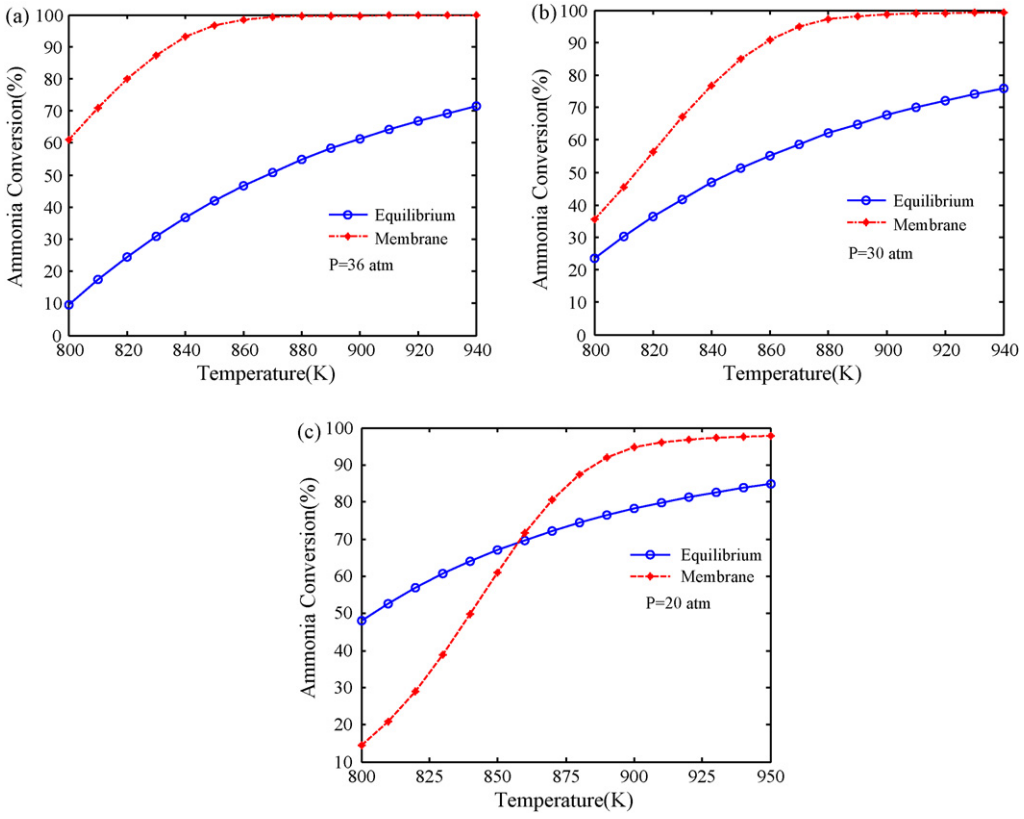

Fig. 3. Comparison of co-current membrane and equilibrium reactors: (a) reaction pressure = 36 atm; (b) reaction pressure = 30 atm; (c) reaction pressure = 20 atm.

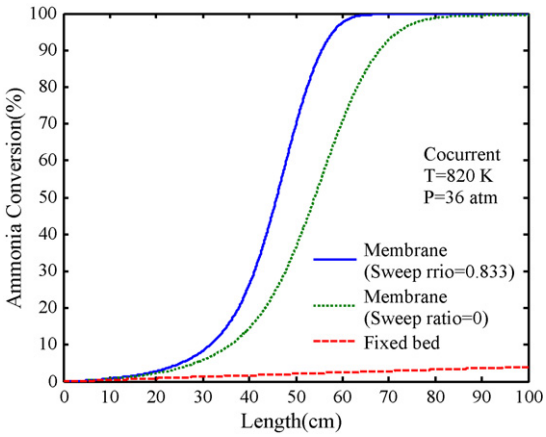

Fig. 4. Comparison of conversion in membrane and fixed bed reactor (no hydrogen permeation).

ammonia conversion in membrane reactor while the equilibrium conversion increases. Hence the membrane reactor approaches to the equilibrium reactor. As the pressure in tube side decreases, the driving force for hydrogen permeation decreases. As a result the conversion in membrane reactor decreases. The result shows that at low pressure and temperature the ammonia conversion in membrane reactor is lower than equilibrium. Fig. 3(c) shows that at pressure of 20 atm and temperature below 860 K under the simulation conditions in Table 2, at the temperature below 860 K, increasing temperature improve the rate of reaction, leading to more conversion of ammonia. As the temperature increases, the positive effect imposed by thermodynamic of endothermic reaction emerges and conversion of ammonia increases, but the ammonia conversion in membrane reactor is lower than equilibrium one since at low temperature and pressure hydrogen permeation decreases and there is not enough residence time for more decomposition of ammonia in the tube side. This phenomenon can be explains according to Daköhler number (*Da*) and permeation number (θ). Tsuru and Yamaguchi [11] presented the effects of Daköhler number (ratio of reaction rate to feed flow rate) and permeation number (ratio of permeation to the feed flow rate) on methane conversion in catalytic membrane reactor for methane steam reforming. In fact, ammonia conversion increases with an increase in Daköhler number (*Da*). The increase in *Da* number, which allows a local equilibrium in the reaction side, as a result of the high reaction rate compared with the feed flow rate, shows the larger conversion. An increase in permeation number θ, which can be achieved either by large hydrogen permeability or by decreasing the feed flow rate, causes a effect on the enhancement of ammonia conversion, therefore ammonia conversion increases beyond the equilibrium conversion when Daköhler number and permeation number increases. The tube lengths used for comparison were 50 cm.

6.2. Comparison between fixed bed and membrane reactor

Fig. 4 shows that ammonia destruction in conventional fixed bed reactor has low efficiency. Since the permeation rate of hydrogen is zero, conversation at these conditions is not more than 5 mol%. In the membrane reactor complete destruction is obtained. Here due to the permeation of hydrogen, the equilibrium shifts to the right and ammonia decomposition occurs. Sweep ratio is defined as the ratio of the flow rate of sweep gas in the shell side to the feed inlet flow rate. Using a sweep gas in shell side decreases the hydrogen partial pressure and increases the driving force for hydrogen permeation. In this figure ammonia conversion for membrane reactor with sweep gas, is higher than the membrane reactor without sweep gas, in other expression a smaller tube length of membrane is required when the sweep gas in the shell side is used.

6.3. Effect of tube side pressure

Fig. 5 shows effect of reaction side pressure on the ammonia conversion along the tube side of membrane reactor. As the tube side pressure increases in both co-current (Fig. 5(a)) and countercurrent (Fig. 5(b)) modes the driving force for hydrogen permeation increases and more hydrogen is removed from reaction side, therefore the equilibrium, shifts to the right and decomposition is gone toward completion. The difference between these modes at high temperature is very insignificant and at low pressure, for example, at 4 atm the ammonia conversion in the outset of reactor is higher than other pressures because the decomposition reaction rate at low pressure is larger

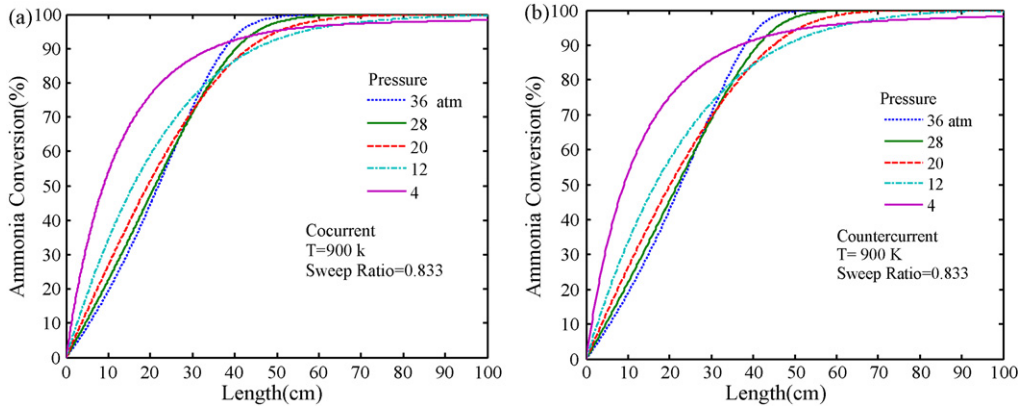

Fig. 5. Effect of pressure on ammonia conversion: (a) co-current flow; (b) countercurrent flow.

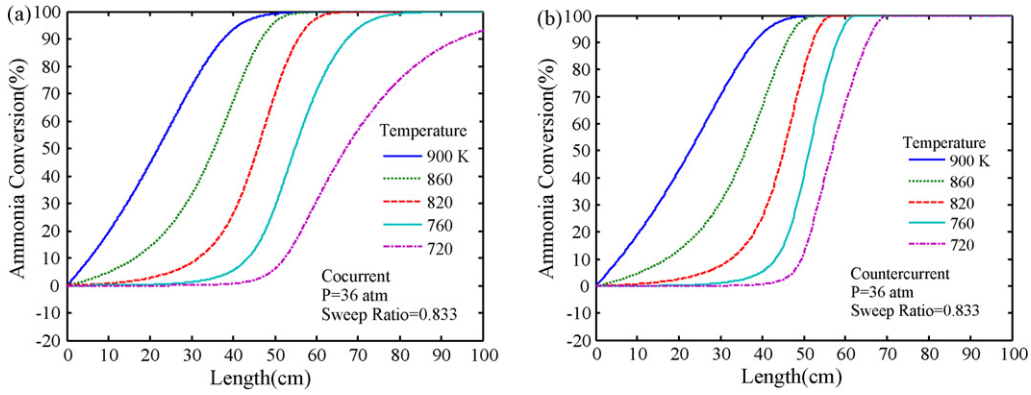

Fig. 6. Effect of temperature on ammonia conversion: (a) co-current flow; (b) countercurrent flow.

but complete destruction of the ammonia cannot be achieved due to lower driving force.

6.4. Effect of tube side temperature

Fig. 6 shows the effect of temperature on the ammonia conversion in catalytic membrane reactor. As temperature increases, the rate of ammonia decomposition and hydrogen permeation increases, therefore ammonia conversion increases. For temperatures below 760 K the difference of conversion between co-current and countercurrent modes will be large and a smaller tube length is required in the countercurrent mode. The major advantage of utilizing a membrane reactor is shown in these figures. At temperature below 760 K an initial increase in the production of ammonia (conversion is negative) occurs, because the concentration of hydrogen and nitrogen are approximately high, but as the hydrogen permeates through the Pd–Ag membrane, the equilibrium is driven toward ammonia decomposition.

6.5. Effect of Pd–Ag membrane thickness

Effect of Pd–Ag layer thickness is shown in Fig. 7. Reducing thickness of Pd–Ag layer raises conversion of ammonia, because the permeation rate of hydrogen is inversely proportional to the layer thickness according to Eq. (4).

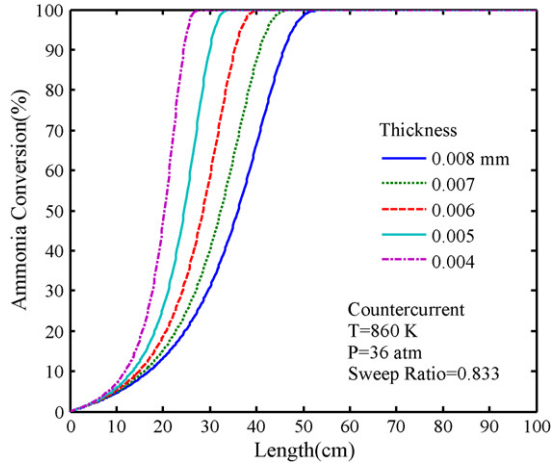

Fig. 7. Effect of thickness of Pd–Ag layer on ammonia conversion (countercurrent flow).

6.6. Effect of reactor diameter

Fig. 8 presents the reactor diameter effect on ammonia conversion in membrane reactor in countercurrent mode. Increasing reactor diameter implements two effects on membrane performance: decreasing space velocity and increasing membrane area. With increasing membrane area, hydrogen more permeate and when the space velocity reduced, there is more residence time for ammonia conversion. Therefore the ammonia conversion rises when the reactor diameter increases.

6.7. Effect of sweep ratio

Fig. 9 demonstrates the effect of sweep ratio on ammonia conversion in countercurrent mode. Sweep ratio defines as the shell side flow rate over tube side flow rate. Increasing shell side flow rate causes increasing sweep ratio and the hydrogen is swept faster and the hydrogen partial pressure reduced. Therefore, hydrogen can more permeate and the ammonia conversion increases.

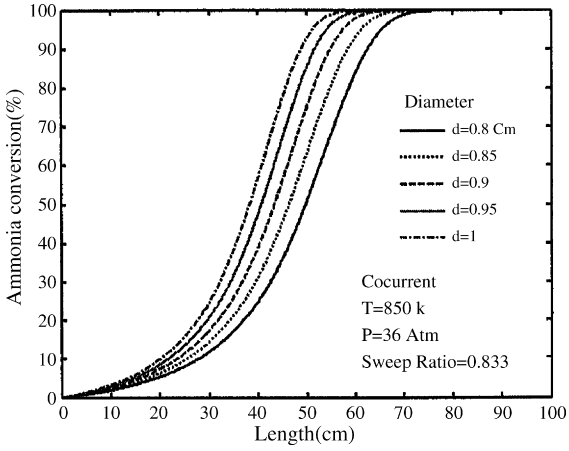

Fig. 8. Effect of reactor diameter on ammonia conversion.

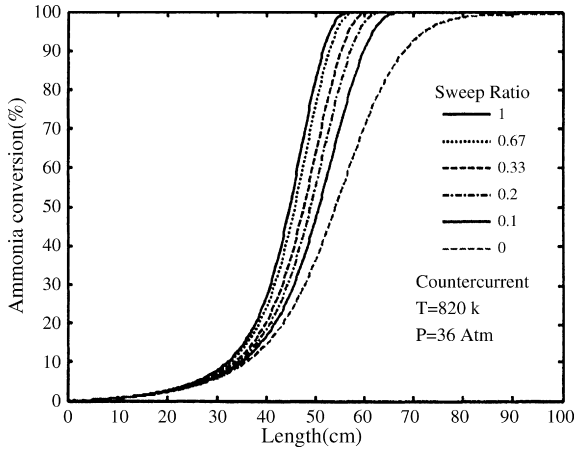

Fig. 9. Effect of sweep ratio on ammonia conversion.

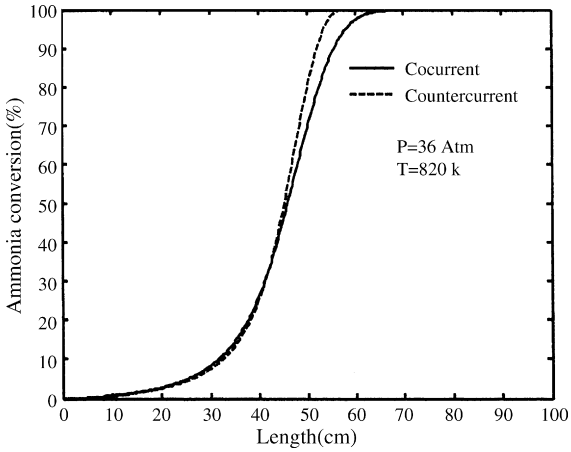

Fig. 12. Comparison of concurrent and countercurrent mode on ammonia conversion.

6.8. Hydrogen recovery

One of the clear advantages of the membrane reactor is hydrogen recovery. Hydrogen recovery is defined as the hydrogen flow rate in shell side to the total hydrogen flow rate in the feed. Fig. 10 shows that at constant pressure but different temperatures, there is very little difference between hydrogen recoveries while at constant temperature and different pressures the deference between hydrogen recoveries is considerable.

6.9. Industrial membrane for complete destruction of ammonia

The purge gas flow rate in Razi petrochemical complex is 570 kg mol/h. In order to utilize this purge gas as fuel in primary reformer, the NH_3 must be removed in industrial catalytic membrane reactor to prevent NO_x formation. The model was used for calculation and the simulation results are in Fig. 11.

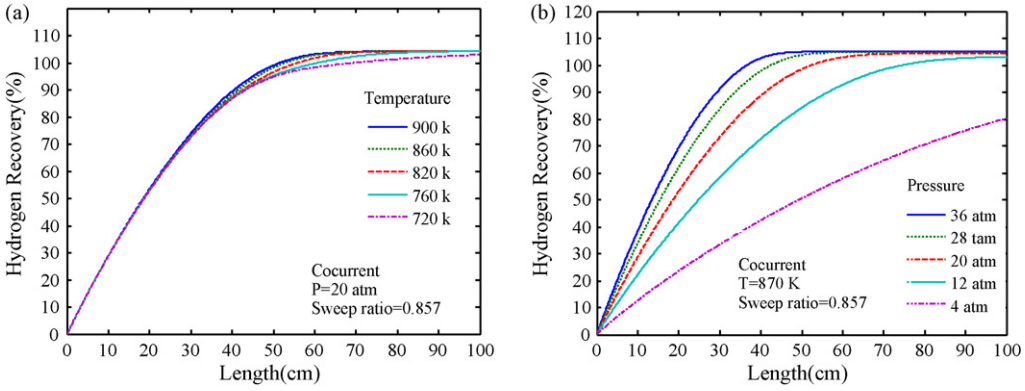

Fig. 10. Effect of temperature (a) and pressure (b) on hydrogen recovery.

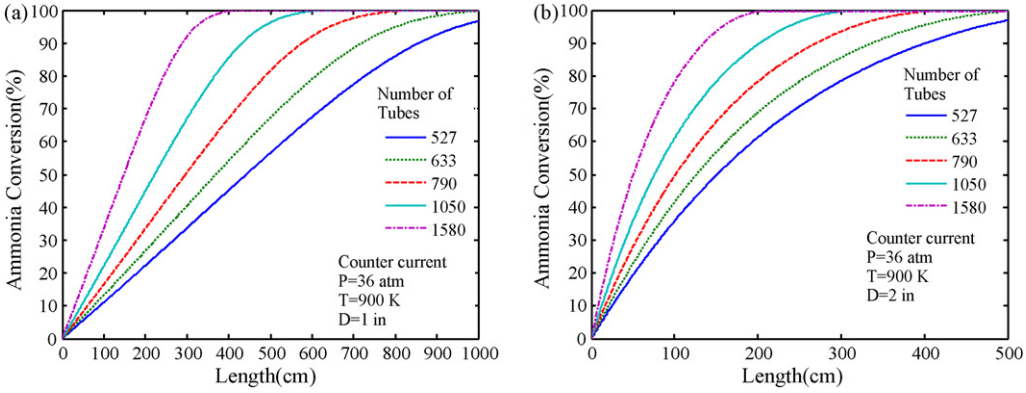

Fig. 11. Calculated specifications of industrial catalytic membrane reactor for elimination of ammonia from purge gases in Razi petrochemical complex: (a) tube diameter = 1 in.; (b) tube diameter = 2 in.

6.10. Comparison of concurrent and countercurrent modes

A comparison of concurrent and countercurrent mode on ammonia conversion has been shown in Fig. 12. This figure illustrates the ammonia conversion at countercurrent mode is higher than co-current mode of operation. As can be seen from this figure, at pressure 36 atm and temperature 820 K, complete conversion takes place at 64 cm for concurrent flow and 55 cm for countercurrent flow. In fact, driving force (difference of hydrogen partial pressure in tube and shell sides) is more in countercurrent mode.

7. Conclusion

A mathematical model was used for simulation of catalytic membrane reactor in order to remove NH_3 from synthesis purge gas of ammonia plant. It has been shown that complete decomposition of NH_3 can be attained by utilizing catalytic membrane reactor, while it is impossible by equilibrium or fixed bed reactor, due to thermodynamics limitation. At lower temperatures (<760 K), the countercurrent mode has superiority compared to co-current mode. Using a sweep gas in the shell side increases the NH_3 decomposition rate. The effects of pressure, temperature, flow rate or sweep ratio, membrane thickness and reactor diameter have been investigated. Generally, it was observed the positive effects on ammonia conversion by increasing the temperature, sweep ratio and reducing membrane thickness. As the tube side pressure increases, more hydrogen is removed from reaction side, therefore the equilibrium, shifts to the right and decomposition is gone toward completion but, at low pressure the ammonia conversion in the outset of reactor is higher than other pressures because the decomposition reaction rate at low pressure is larger but complete destruction of the ammonia cannot be achieved due to lower driving force. An additional potential membrane reactor application is the recovery of H_2 from purge gas mixer that can be used as fuel. Use of such system would be important for the prevention of NO_x emission, global warming and acid rain which at present time have a significant environmental impact. Combining reaction and separation in a single unit operation, low energy consumption and smaller reactor length are other advantages of a catalytic membrane reactor.

References

[1] T.-L. Huang, K.R. Cliffe, J.M. Mainnes, The removal of ammonia from water by a hydrophobic catalyst, Environ. Sci. Technol. 34 (2000) 4804–4809.

[2] National Pollutant Inventory (NPI), Ammonia Fact Sheet (Ammonia Total), version 1.0, April 2007.

[3] Razi Petrochemical Complex, Ammonia Plant Operating Data, 2006.

[4] E.N. Gobina, J.S. Oklany, R. Houghes, Elimination of ammonia from coal gasification streams by using a catalytic membrane reactor, Ind. Eng. Chem. Res. 34 (1995) 3777–3783.

[5] Shiraz Petrochemical Complex, Argon and Hydrogen Recovery Unit Operating Manual, 1991.

[6] M.R. Rahimpour, M. Lotfinejad, Enhancement of methanol production in a membrane dual-type reactor, Chem. Eng. Technol. 30 (8) (2007) 1062–1076.

[7] R. Dittmeyer, V. Höllein, K. Daub, Membrane reactors for hydrogenation and dehydrogenation processes based on supported palladium, J. Mol. Catal. A: Chem. 173 (2001) 135–184.

[8] R.E. Buxbaum, A.B. Kinney, Hydrogen transport through tubular membranes of palladium-coated tantalum and niobium, Ind. Eng. Chem. Res. 35 (1996) 530.

[9] J. Shu, B.P.A. Grandjean, S. Kaliaguine, Asymmetric Pd–Ag/stainless steel catalytic membranes for methane steam reforming, Catal. Today 25 (1995) 327–332.

[10] F. Gallucci, L. Paturzo, A. Basile, A simulation study of the steam reforming of methane in a dense tubular membrane reactor, Int. J. Hydrogen Energy 29 (2004) 611–617.

[11] P. Hacarlioglu, Y. Gu, S.T. Oyama, Studies of the methane steam reforming reaction at high pressure in a ceramic membrane reactor, J. Nat. Gas Chem. 15 (2006) 73–81.

[12] T. Tsuru, K. Yamaguchi, T. Yoshioka, M. Asaeda, Methane steam reforming by microporous catalytic membrane reactors, AIChE J. 50 (2004) 2794–2805.

[13] E. Gobina, R. Hughes, Ethane dehydrogenation using a high-temperature catalytic membrane reactor, J. Membr. Sci. 90 (1994) 11–19.

[14] J.N. Keuler, L. Lorenzen, Comparing and modeling the dehydrogenation of Ethanol in a plug flow reactor and a Pd–Ag membrane reactor, Ind. Eng. Chem. Res. 41 (2002) 1960–1966.

[15] B.S. Liu, W.D. Zhang, W.L. Dai, J.F. Deng, Thermal stability, hydrogen adsorption and separation performance of Ni-based amorphous alloy membranes, J. Membr. Sci. 244 (2004) 243–249.

[16] M.R. Rahimpour, S. Ghader, Enhancement of CO conversion in a novel Pd–Ag membrane reactor for methanol synthesis, Chem. Eng. Process. 43 (2004) 1181–1188.

[17] M.R. Rahimpour, S. Ghader, Theoretical investigation of a Pd-membrane reactor for methanol synthesis, Chem. Eng. Technol. 26 (8) (2003)902.

[18] R.C. Hurlburt, J.O. Konency, Diffusion of hydrogen through palladium, J. Chem. Phys. 34 (1961) 655–658.

[19] F.J. Ackerman, G.J. Koskinas, Permeation of hydrogen and deuterium through palladium–silver alloys, J. Chem. Eng. Data 17 (1972) 51–55.

[20] H. Yoshida, S. Konishi, Y. Naruse, Effects of impurities on hydrogen permeability through palladium alloy, J. Less-Common Met. 89 (1983) 429–436.

[21] J. Chabot, J. Lecomte, C. Grumet, J. Sannier, Fuel clean-up system. Poisoning of palladium–silver membranes by gaseous impurities, Fusion Technol. 14 (1988) 614–618.

[22] M. Temkin, V. Pyzhev, Kinetics of the synthesis of ammonia on promoted iron catalysts, Acta Physicochim. URRS 12 (1940) 327.

[23] A. Nielsen, J. Kjaer, B.L. Hansen, Rate equation and mechanism of ammonia synthesis at industrial conditions, J. Catal. 3 (1964) 68–79.

[24] C.N. Satterfield, Heterogeneous Catalysis in Practice, McGraw-Hill, New York, NY, 1980.

[25] J.P. Collins, J.D. Way, N. Kraisuwansarn, A mathematical model of a catalytic membrane reactor for the decomposition of NH_3, J. Membr. Sci. 77 (1993) 265–282.

[26] R.H. Harrison, K.A. Kobe, Thermodynamics of ammonia synthesis and oxidation, Chem. Eng. Prog. 49 (1953) 349–353.

[27] E. Gobina, K. Hou, R. Hughes, Ethane dehydrogenation in a catalytic membrane reactor coupled with a reactive sweep gas, Chem. Eng. Sci. 50 (July (14)) (1995) 2311–2319.

[28] E. Gobina, K. Hou, R. Hughes, Mathematical analysis of ethylbenzene dehydrogenation: comparison of microporous and dense membrane systems, J. Membr. Sci. 105 (September (3)) (1995) 163–176.

[29] A. Constantinides, N. Mostoufi, Numerical Methods for Chemical Engineers With MATLAB Applications, Nashr-e Ketab-e Daneshgahi, Tehran, 2001.